Instability of plane-parallel flow of incompressible liquid over a saturated porous medium

T. P. Lyubimova,[1,2] D. V. Lyubimov,[2] D. T. Baydina,[2] E. A. Kolchanova,[1,2] and K. B. Tsiberkin[1,2]
[1]*Institute of Continuous Media Mechanics, Ural Branch of RAS, Perm, Russia*
[2]*Perm State University, Theoretical Physics Department, Perm, Russia*
(Received 27 November 2015; revised manuscript received 5 May 2016; published 7 July 2016)

The linear stability of plane-parallel flow of an incompressible viscous fluid over a saturated porous layer is studied to model the instability of water flow in a river over aquatic plants. The saturated porous layer is bounded from below by a rigid plate and the pure fluid layer has a free, undeformable upper boundary. A small inclination of the layers is imposed to simulate the riverbed slope. The layers are inclined at a small angle to the horizon. The problem is studied within two models: the Brinkman model with the boundary conditions by Ochoa-Tapia and Whitaker at the interface, and the Darcy-Forchheimer model with the conditions by Beavers and Joseph. The neutral curves and critical Reynolds numbers are calculated for various porous layer permeabilities and relative thicknesses of the porous layer. The results obtained within the two models are compared and analyzed.

DOI: 10.1103/PhysRevE.94.013104

I. INTRODUCTION

The flow over a saturated porous layer captures the fluid inside it. The large drag force in a porous medium leads to rapid reduction of the horizontal velocity of flow. This, it its turn, results in instability similar to the Kelvin-Helmholtz instability: the vortex motion occurs near the interface and mixes the fluid.

The above phenomenon is widely studied. The most classical formulation is the problem of an incompressible fluid flow bounded by a rigid wall from above and by an infinite porous layer from below, under a horizontal pressure gradient [1,2]. There are also several works on similar flow in the layer bounded by the finite-thickness porous layers from both sides, e.g., [3,4].

The described instability is very important for many applications. It may cause contaminant surges from the water or ground plants. It is known that the aquatic plants or forest canopy slows down the river flow or wind and captures the contaminants from the surrounded medium. In this case the instability leads to the rapid flow acceleration in the porous layer and the contaminants can be ejected to the external flow [5,6]. This can be significant for regions with a severe environmental situation.

Another important application is the study of the melt flow near the solidification front. During directional solidification of binary melts the two-phase zone (mushy zone) is formed near the melt-crystal interface and the flow in this zone has significant influence on the crystal quality. The peculiarities of the convective flows in systems consisting of the homogeneous fluid layer and saturated porous medium are investigated in [7–13]. The linear stability criteria and nonlinear dynamics of laminar whirl flows which correspond to two main instability modes are presented in [8]. A similar problem for Oldroyd-B non-Newtonian fluid is studied in [9]. A number of papers are devoted to the complex factors effects on the two-layer system dynamics, e.g., magnetic fields [10,11], solutal convection [12], and transversal fluid pumping [13].

The flow stability problem associated with the thermal flux through the interface is studied in [14]. It is applicable for fuel cell development, biological materials flow studies, etc. [2].

A unique feature of multilayer systems of liquid and saturated porous medium is the bimodality of neutral stability curves which correspond to two independent instability mechanisms [2,4,8,10–12,15,16]. The first mechanism leads to the formation of large-scale, large-wavelength vortices which cover the entire system. The second mechanism results in the development of short-wave vortices localized near the interface. The bimodality of neutral curves was discovered in study of the convection in a three-layer system of liquid and a porous medium [15].

There are many different theoretical models of filtration flow and boundary conditions at the interface of pure fluid and saturated porous medium [1,14,17–19]. In [20,21] the improvement of the approach by Ochoa-Tapia and Whitaker [17,18] is suggested. Momentum transfer through the interface is important for theoretical fluid mechanics as well as for its applications [1,2,4,14,17–23]. The three-layer system consisting of the Darcy porous layer, homogeneous fluid layer, and thin transitional Brinkman porous layer between them is described in [24].

In the present paper, we analyze the linear stability of stationary plane-parallel flow of homogeneous fluid over the saturated porous medium in the framework of different filtration models with corresponding boundary conditions at the interface of the porous medium and overlying fluid. The motivation of our work is the analysis of instability of flow over aquatic plants which is why, different from the papers [1–4] where the flow induced by horizontal pressure gradient was considered, we introduce a small inclination of the layers to imitate the riverbed slope.

The study uses two models. The first model is based on the Brinkman model. It uses the interface boundary conditions for the viscous stresses proposed by Ochoa-Tapia and Whitaker [17,18]. These conditions lead to the tangential stress jump and break of stationary velocity profile at the interface. The second model uses the Darcy and Darcy-Forchheimer equations with the boundary condition at the interface suggested by Beavers and Joseph [19]. In this case there is a tangential velocity jump at the interface.

The linear stability of fluid flow over the saturated porous medium was studied earlier in [25] using the "one-equation" model. The two-layer system was treated as a single fluid-saturated porous layer with the nonuniform porosity and permeability sharply changing at the coordinate which corresponds to the interface location.

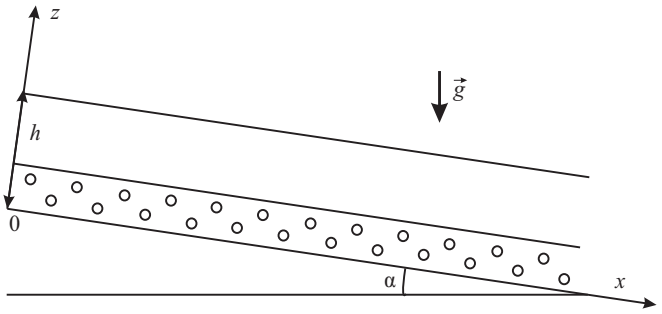

FIG. 1. Two-layer system geometry.

There are some very recent papers where similar problems are studied for different structures of stationary flow. In [26] the stability of plane-parallel shear flow over the porous medium is studied within the model with variable porosity changing from some value to unity in the transition layer between the Brinkman porous medium and the overlying pure fluid. It is shown that in this case the shear flow is always unstable and instability develops near the interface of the porous layer and the transition zone. In [27,28] granular bed erosion by a channel flow is investigated.

The paper is organized as follows. Physical models and boundary conditions are described in Sec. II. The linear stability results are presented in Sec. III. The general properties of the solutions and the instability mechanisms are discussed in Sec. IV. Section V contains concluding remarks.

II. FILTRATION MODELS, GOVERNING EQUATIONS, AND BOUNDARY CONDITIONS AT THE INTERFACE

A. Problem geometry

We study the two-layer system consisting of a viscous incompressible fluid overlying the porous medium saturated by the same fluid (Fig. 1). The lower boundary of the layer is rigid and impermeable for the fluid and the upper boundary is free and undeformable. The interface is flat and undeformable. We consider the two-dimensional problem uniform in the y direction. The riverbed slope is modeled by the layers' slope at the angle α to the horizon, and the fluid flows down due to the gravity force. There is no longitudinal pumping. We use two filtration models described below.

B. Brinkman model

In the first model the Navier-Stokes equations describe the flow in the layer of viscous incompressible fluid:

$$\frac{\partial \vec{v}}{\partial t} + (\vec{v}\cdot\vec{\nabla})\vec{v} = -\frac{\vec{\nabla} p}{\rho} + \nu\nabla^2\vec{v} - g\vec{\gamma}, \tag{1}$$

$$\vec{\nabla}\cdot\vec{v} = 0, \tag{2}$$

while the governing equations in the saturated porous layer are as follows:

$$\frac{\partial \vec{v}_p}{\partial t} + (\vec{v}_p\cdot\vec{\nabla})\vec{v}_p = -\frac{\vec{\nabla} p_p}{\rho} - \frac{\nu}{K}\varphi\vec{v}_p + \tilde{\nu}\varphi\nabla^2\vec{v}_p - g\vec{\gamma}, \tag{3}$$

$$\vec{\nabla}\cdot\vec{v}_p = 0, \tag{4}$$

where $\vec{v}$ is the velocity of the overlying fluid, $\vec{v}_p$ is the velocity of the flow in the pores, p is the pressure φ, K is the porosity and permeability, ρ and ν are the density and kinematic viscosity of the fluid, $\tilde{\nu}$ is the effective kinematic viscosity in the porous layer, $\vec{g} = -g\vec{\gamma}$ is the gravity acceleration, and $\vec{\gamma}$ is the unit vector directed vertically upward. Here, the variables with subscript p denote the porous medium, while the variables without subscripts mark the pure fluid.

The momentum equation for the porous medium (3) is based on the Brinkman model. It contains the porous matrix drag force (Darcy-like term) and the additional term describing the momentum diffusion. The quantity $\tilde{\nu}$ depends on the properties of the porous medium. There are some studies where it is assumed that $\tilde{\nu} > \nu$ and their ratio grows monotonically with porosity decrease (see, e.g., [17,18,24]). According to [17,18] we assume

$$\frac{\tilde{\nu}}{\nu} = \frac{1}{\varphi}.$$

The Brinkman model well describes the behavior of highly permeable media with high porosity [29,30]. Some authors note that the minimal porosity value when the momentum diffusion should be taken into account is $\varphi = 0.6$ [1]. We use this value and study the intermediate range of parameters where both the Brinkman model and the Darcy model can be applied.

The governing equations (1)–(4) are completed with the following boundary conditions. We set the impermeability and tangential stress absence conditions at the upper nondeformable boundary, and the no-slip condition at the lower boundary:

$$\begin{aligned} &z = h: v_z = 0, \quad \frac{\partial v_x}{\partial z} + \frac{\partial v_z}{\partial x} = 0, \\ &z = 0: \vec{v}_p = 0. \end{aligned} \tag{5}$$

The boundary conditions suggested by Ochoa-Tapia and Whitaker [17,18] are imposed at the interface:

$$\begin{aligned} z = h_1: \ &\vec{v} = \varphi\vec{v}_p, \\ -p + 2\nu\rho\frac{\partial v_z}{\partial z} &= -p_p + 2\tilde{\nu}\rho\varphi\frac{\partial v_{pz}}{\partial z}, \\ \frac{\partial v_x}{\partial z} - \frac{\tilde{\nu}}{\nu}\varphi\frac{\partial v_{px}}{\partial z} &= -\frac{\beta_{\mathrm{OTW}}}{K^{1/2}}\varphi v_{px}, \end{aligned} \tag{6}$$

where h_1 is the porous layer thickness and β_{OTW} is the dimensionless coefficient depending on the material parameters of porous medium and fluid near the interface [17,18]. These conditions include the continuity of the velocity components and normal stresses, and the jump of tangential stresses describing the resistance of porous matrix in the boundary layer whose thickness is of the order of $K^{1/2}$. For real systems the values of β_{OTW} are close to unity [18]. At $\beta_{\mathrm{OTW}} = 0$ the tangential stress jump condition is transformed into the tangential stress continuity condition proposed in [15]. The conditions (6) were obtained by strict mathematical procedure from the Navier-Stokes equations at pore scale; nevertheless, they include the empirical parameter β [1,7,19]. Note that the boundary conditions by le Bars and Worster result in a similar

velocity profile within the Darcy model [7]' however, in our work these conditions are not analyzed.

We use the following scales:

$$[\vec{r}] = h, \quad [t] = \frac{h^2}{\nu}, \quad [U] = \frac{gh^2}{\nu}\sin\alpha, \quad [p] = \rho g h \sin\alpha,$$

i.e., the full system thickness for the length, the double maximal velocity of the fluid flowing down the impermeable inclined plate for the velocity, the viscous time scale for the time, and the hydrostatic pressure along the inclined layer for pressure.

The dimensionless equations and boundary conditions are as follows:

$$\frac{\partial \vec{v}}{\partial t} + \mathrm{Re}(\vec{v}\cdot\vec{\nabla})\vec{v} = -\vec{\nabla}p + \nabla^2\vec{v} - \frac{1}{\sin\alpha}\vec{\gamma}, \tag{7}$$

$$\vec{\nabla}\cdot\vec{v} = 0, \tag{8}$$

$$\frac{\partial \vec{v}_p}{\partial t} + \mathrm{Re}(\vec{v}_p\cdot\vec{\nabla})\vec{v}_p = -\vec{\nabla}p_p - q^2\varphi\vec{v}_p + \nabla^2\vec{v}_p - \frac{1}{\sin\alpha}\vec{\gamma}, \tag{9}$$

$$\vec{\nabla}\cdot\vec{v}_p = 0, \tag{10}$$

$$\begin{aligned} &z = 1 : v_z = 0, \quad \frac{\partial v_x}{\partial z} + \frac{\partial v_z}{\partial x} = 0, \\ &z = 0 : \vec{v}_p = 0, \end{aligned} \tag{11}$$

$$\begin{aligned} &z = d : \vec{v} = \varphi\vec{v}_p, \quad -p + 2\frac{\partial v_z}{\partial z} = -p_p + 2\varphi\frac{\partial v_{pz}}{\partial z}, \\ &\frac{\partial v_x}{\partial z} - \frac{\partial v_{px}}{\partial z} = -\beta_{\mathrm{OTW}} q \varphi v_{px}. \end{aligned} \tag{12}$$

The equation system (7)–(10) is nonlinear for the both layers, while the boundary conditions are linear. Additional nonlinearity occurs at $\beta_{\mathrm{OTW}} \neq 0$. It corresponds to the tangential viscous stresses jump at the interface.

The problem contains the following dimensionless parameters: Reynolds number, Darcy number, and relative thickness of the porous layer:

$$\mathrm{Re} = \frac{Uh}{\nu} = \frac{gh^3}{\nu^2}\sin\alpha, \quad \mathrm{Da} = \frac{K}{h^2}, \quad d = \frac{h_1}{h}.$$

We also use the parameter $\mathrm{q} = \mathrm{Da}^{-1/2}$.

C. Darcy-Forchheimer model

In the second model, the Navier-Stokes equations describe the flow of the viscous incompressible fluid:

$$\frac{\partial \vec{v}}{\partial t} + (\vec{v}\cdot\vec{\nabla})\vec{v} = -\frac{\vec{\nabla}p}{\rho} + \nu\nabla^2\vec{v} - g\vec{\gamma}, \tag{13}$$

$$\vec{\nabla}\cdot\vec{v} = 0, \tag{14}$$

while the flow in the porous layer is described by the Darcy-Forchheimer law extension [1]:

$$\frac{\partial \vec{v}_p}{\partial t} + (\vec{v}_p\cdot\vec{\nabla})\vec{v}_p = -\frac{\vec{\nabla}p_p}{\rho} - \frac{\nu}{K}\varphi\vec{v}_p - \varphi^2\frac{c_F}{K^{1/2}}|\vec{v}_p|\vec{v}_p - g\vec{\gamma}, \tag{15}$$

$$\vec{\nabla}\cdot\vec{v}_p = 0, \tag{16}$$

where $c_F \approx 0.55$ is the universal Forchheimer constant. The variables with subscript p denote the porous medium, while the variables without subscripts mark the pure fluid, as in the previous section.

The Forchheimer term is important when the pore-scale Reynolds number Re_p is of the order 1–10 and higher [1]. For the problem under consideration, the largest values of Re_p are of the order 10^2–10^3 which is outside the Darcy law validity range; however, accounting for the nonlinear Forchheimer force partially compensates for this. For the lowest permeability values in the problem under consideration the values of Re_p are of the order 10^1–10^2; therefore it is possible to use both the Darcy law and the Darcy-Forchheimer extension with sufficient accuracy. Thus, both approaches should be adequate for the problem under consideration.

We set the impermeability and tangential stress absence conditions at the upper nondeformable boundary, and the impermeability condition at the lower boundary:

$$\begin{aligned} &z = h : v_z = 0, \quad \frac{\partial v_x}{\partial z} + \frac{\partial v_z}{\partial x} = 0, \\ &z = 0 : v_{pz} = 0. \end{aligned} \tag{17}$$

The boundary conditions at the interface contain the continuity of normal velocity components and pressure in both layers and the condition for the tangential velocity components suggested by Beavers and Joseph [19]:

$$z{=}h_1 : v_z = \varphi v_{p_z}, \quad p = p_p, \quad \frac{\partial v_x}{\partial z} = \frac{\alpha_{\mathrm{BJ}}}{K^{1/2}}(v_x - \varphi v_{px}), \tag{18}$$

where α_{BJ} is the dimensionless coefficient depending on the parameters of a porous medium and fluid [19]. The Darcy model leads to the differential equation system of sixth order unlike the eighth-order system in the Brinkman model. Therefore, the Darcy model requires a lower number of boundary conditions, and the conditions by Beavers and Joseph should be used here [1,7].

An important distinction of the second model is the absence of the direct boundary conditions for the tangential and normal stresses at the interface. The conditions by Beavers and Joseph are empirical [19] but they provide completeness for the problem. One should use these conditions since the plane-parallel flow velocities found from the Darcy and Darcy-Forchheimer laws do not depend on the z coordinate. It is a result of the structure of filtration equation (15), which is algebraic with respect to the velocity. Note that the simplified form of the boundary conditions (18) suggested by Saffman [1] could be obtained by the strict procedure from the Navier-Stokes equations at the pore scale [31].

Using the same scales as in the previous subsection, we obtain the governing equations in the form

$$\frac{\partial \vec{v}}{\partial t} + \mathrm{Re}(\vec{v}\cdot\vec{\nabla})\vec{v} = -\vec{\nabla}p + \nabla^2\vec{v} - \frac{1}{\sin\alpha}\vec{\gamma}, \tag{19}$$

$$\vec{\nabla}\cdot\vec{v}=0, \tag{20}$$

$$\frac{\partial\vec{v}_p}{\partial t}+\mathrm{Re}(\vec{v}_p\cdot\vec{\nabla})\vec{v}_p = -\vec{\nabla}p_p-q^2\varphi\vec{v}_p-q\varphi^2c_F\mathrm{Re}|\vec{v}_p|\vec{v}_p-\frac{1}{\sin\alpha}\vec{\gamma}, \tag{21}$$

$$\vec{\nabla}\cdot\vec{v}_p=0, \tag{22}$$

with boundary conditions

$$z=1: v_z=0,\quad \frac{\partial v_x}{\partial z}+\frac{\partial v_z}{\partial x}=0,$$
$$z=0: v_{pz}=0, \tag{23}$$
$$z=d: v_z=\varphi v_{p_z},\quad p=p_p,\quad \frac{\partial v_x}{\partial z}=\alpha_{\mathrm{BJ}}q(v_x-\varphi v_{px}).$$

The dimensionless parameters are the same as in the Brinkman model.

D. Stationary flow

For both models described above the problem has an analytical stationary solution. It corresponds to the plane-parallel flow with a zeroth z component of the velocity.

The equations for stationary plane-parallel flow in the fluid layer overlying the porous medium are as follows:

$$-\frac{\partial p_0}{\partial x}+\frac{\partial^2U}{\partial z^2}+1=0, \tag{24}$$

$$-\frac{\partial p_0}{\partial z}-\cot\alpha=0. \tag{25}$$

They are the same for the Darcy and Brinkman models.

Projection of the stationary plane-parallel filtration equation to the x axis in the Brinkman model is as follows:

$$\frac{\partial p_0}{\partial x}=\frac{\partial^2U_p}{\partial z^2}-q^2\varphi U_p+1, \tag{26}$$

and in the Darcy-Forchheimer equation it is

$$-\frac{\partial p_0}{\partial x}-q^2\varphi U_p-q\varphi^2c_F\mathrm{Re}U_p^2+1=0. \tag{27}$$

Finally, the z-axis projection of the filtration equation is the same for both models and it coincides with (25).

For the problem under consideration the only source of flow is the gravity force; the x component of the pressure gradient equals zero and stationary vertical pressure distribution is unified in the pure fluid and saturated porous layer. Taking the pressure at the free upper boundary as the reference value, we obtain

$$p_0(z)=(1-z)\cot\alpha. \tag{28}$$

The filtration velocity in the Brinkman model is as follows:

$$\varphi U_p(z)=2A\varphi\sinh rz-\frac{\varphi}{r^2}(\mathrm{e}^{-rz}-1), \tag{29}$$

where

$$A=\frac{1-d-r^{-1}\mathrm{e}^{-rd}-\beta_{\mathrm{OTW}}q^{-1}(\mathrm{e}^{-rd}-1)}{2(r\cosh rd-\beta_{\mathrm{OTW}}q\varphi\sinh rd)},$$

and the parameter $r=q\varphi^{1/2}$ is introduced to shorten the notation. The velocity profile in the overlying fluid is

$$U(z)=(z-d)-\frac{z^2-d^2}{2}+2A\varphi\sinh rd-\frac{\varphi}{r^2}(\mathrm{e}^{-rd}-1). \tag{30}$$

The filtration velocity U_p in the Darcy-Forchheimer model is determined by (27)

$$U_p=\frac{1}{2\varphi c_Fq\mathrm{Re}}\left[\left(1+\frac{4c_F\mathrm{Re}}{q^3}\right)^{1/2}-1\right]. \tag{31}$$

Neglecting the Forchheimer force, one reduces Eq. (31) to the well-known result [1],

$$U_p^{\mathrm{Da}}=\frac{1}{q^2\varphi}. \tag{32}$$

The filtration velocity does not depend on the coordinate in the porous layer due to the structure of Eqs. (26) and (27) for the velocity. The velocity profile in pure fluid is parabolic and the Beavers and Joseph boundary condition leads to some shift of the velocity:

$$U(z)=(z-d)-\frac{z^2-d^2}{2}+\frac{1-d}{\alpha_{\mathrm{BJ}}q}+\varphi U_p. \tag{33}$$

Figure 2 presents the stationary plane-parallel flow profiles calculated for the porosity $\varphi=0.6$ and different values of the other parameters. One can see that there is a large difference in the velocity profiles for different models [14]: The velocity profile has a break at the interface in the Brinkman model, while the velocity jump exists in the Darcy-Forchheimer model. This has principal influence on the flow stability.

III. LINEAR STABILITY ANALYSIS

In this section we present the results of linear stability analysis of plane-parallel stationary flow of fluid over the saturated porous medium for the Brinkman and Darcy-Forchheimer model. Discussion of the results, and comparative analysis of the models, different instability mechanisms, and the influence of the parameter values on the stability characteristics are included in Sec. IV.

A. Brinkman model

Let us proceed to the investigation of the stationary flow stability in different filtration models. We begin from the Brinkman model. We present the velocity and pressure in both layers as the sums of stationary solutions and small perturbations:

$$\vec{v}=\vec{U}+\vec{v}',\quad p=p_0+p', \tag{34}$$

Substituting (34) into Eqs. (7)–(10) and boundary conditions (11) and (12) and neglecting the terms of second order of smallness we obtain linearized equations for perturbations in the form

$$\frac{\partial\vec{v}'}{\partial t}+\mathrm{Re}[(\vec{U}\cdot\vec{\nabla})\vec{v}'+(\vec{v}'\cdot\vec{\nabla})\vec{U}]=-\vec{\nabla}p'+\nabla^2\vec{v}', \tag{35}$$

$$\vec{\nabla}\cdot\vec{v}'=0, \tag{36}$$

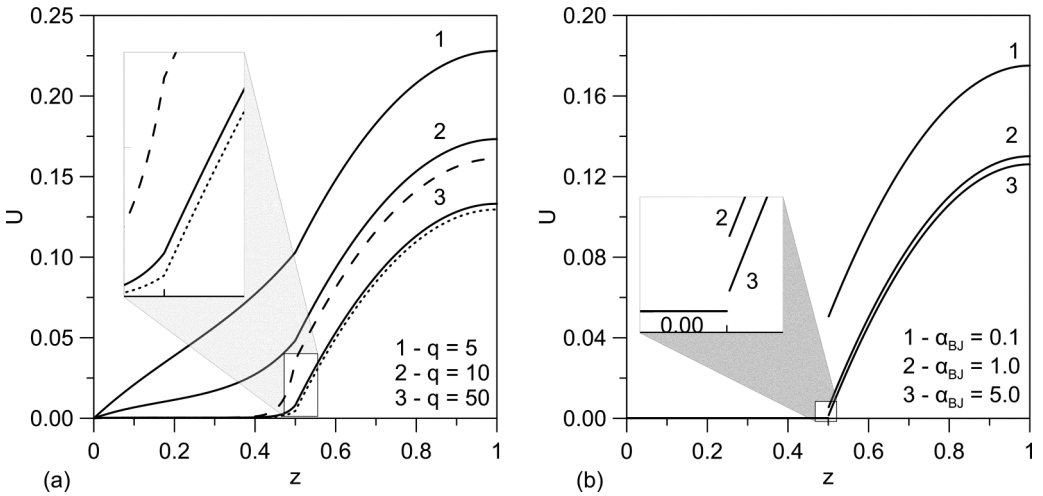

FIG. 2. Velocity profiles for stationary flows in two-layer system: (a) for the Brinkman model with boundary conditions by Ochoa-Tapia and Whitaker at the interface for $d = 0.5, \beta_{\mathrm{OTW}} = 0$ (solid lines), $\beta_{\mathrm{OTW}} = -1$ (dotted lines), $\beta_{\mathrm{OTW}} = +1$ (dashed lines); (b) for the Darcy model with the boundary conditions by Beavers and Joseph at the interface for $d = 0.5, q = 100(\mathrm{Da} = 1 \times 10^{-4})$.

$$\frac{\partial \vec{v}'_p}{\partial t} + \mathrm{Re}[(\vec{U}_p \cdot \vec{\nabla})\vec{v}'_p + (\vec{v}'_p \cdot \vec{\nabla})\vec{U}_p] = -\vec{\nabla} p'_p - q^2 \varphi \vec{v}'_p + \nabla^2 \vec{v}'_p, \tag{37}$$

$$\vec{\nabla} \cdot \vec{v}'_p = 0. \tag{38}$$

The boundary conditions (11) and (12) do not change their form due to their linearity. The primes are omitted further below.

Applying curl_y to Eqs. (35) and (37) and using the continuity equations we exclude the pressure and x components of the velocities. By introducing normal-mode perturbations $w, \Omega \sim \exp(\lambda t + ikx)$ we obtain the system of equations where all the variables are functions of the z coordinate only:

$$\lambda\Omega + \mathrm{Re}(ikU\Omega + wU'') = \Omega'' - k^2\Omega, \tag{39}$$

$$w'' - k^2 w = ik\Omega, \tag{40}$$

$$\lambda\Omega_p + \mathrm{Re}(ikU_p\Omega_p + w_p U''_p) = -q^2\varphi\Omega_p + \Omega''_p - k^2\Omega_p, \tag{41}$$

$$w''_p - k^2 w_p = ik\Omega_p, \tag{42}$$

with the boundary conditions

$$\begin{aligned} &z = 0: \ w_p = w'_p = 0, \\ &z = 1: w = w'' = 0, \\ &z = d: w = \varphi w_p, \quad w' = \varphi w'_p, \\ &(\lambda + 2k^2)(w' - w'_p) + ik\mathrm{Re}(Uw' - U_p w'_p) \\ &\quad - ik\mathrm{Re}(U'w - U'_p w_p) + ik\Omega' = q^2\varphi w'_p + ik\Omega'_p, \\ &ik(\Omega - \Omega_p) - k^2(w - w_p) = \beta_{\mathrm{OTW}} q \varphi w'_p. \end{aligned} \tag{43}$$

where w, w_p are the z components of the velocities and Ω, Ω_p are the y components of the vorticities.

The linear stability problem (39)–(43) was solved numerically by a shooting method based on the calculation of the fundamental system solution with step-by-step orthogonalization of the solution vectors [32,33]. After the critical values of parameters have been obtained, the critical motions are calculated by the direct integration of the linear stability equations.

Figure 3 shows the neutral and dispersion curves for $d = 0.35$ and different values of q, and Fig. 4—for $q = 150$ and different values of d. As one can see, the permeability reduction or q growth increases the instability threshold. The critical Reynolds number well corresponds to the results from [4] after variable rescaling. It verifies our approach, because the authors [4] apply the collocation method with a large number of solution expansion components. At the same time, the study in [4] is performed for a narrow permeability value range near $q = 100(\mathrm{Da} \sim 10^{-4})$, and there is no detailed study of the neutral curves transformation with the parameter change.

Figures 5(a) and 5(b) illustrate the structure of critical perturbations for long-wave and short-wave modes (the real and imaginary parts of the vertical component of perturbation velocity for the parameter values close to the long-wave and short-wave minima of the neutral curve at $d = 0.5$, $q = 170$ are plotted).

The critical Reynolds number dependence on the porous layer thickness is nonmonotonic. For $d < 0.6$, the global minimum of the neutral curve decreases with d growth due to the long-wave minimum lowering. If $d > 0.6$, the system becomes more stable due to the long-wave minimum displacement upward. The short-wave minimum increases and is smoothing with d growth, such that at large d the neutral curve is unimodal.

Figure 6 illustrates the influence of the parameter β_{OTW} on flow stability. We study β_{OTW} in the interval from –1 to +1. It corresponds to its values obtained in [18] from the experimental and theoretical data comparison. This parameter determines the tangential stress jump at the interface. As one can see, the system is very sensitive to the change of the interfacial boundary condition. The most significant changes

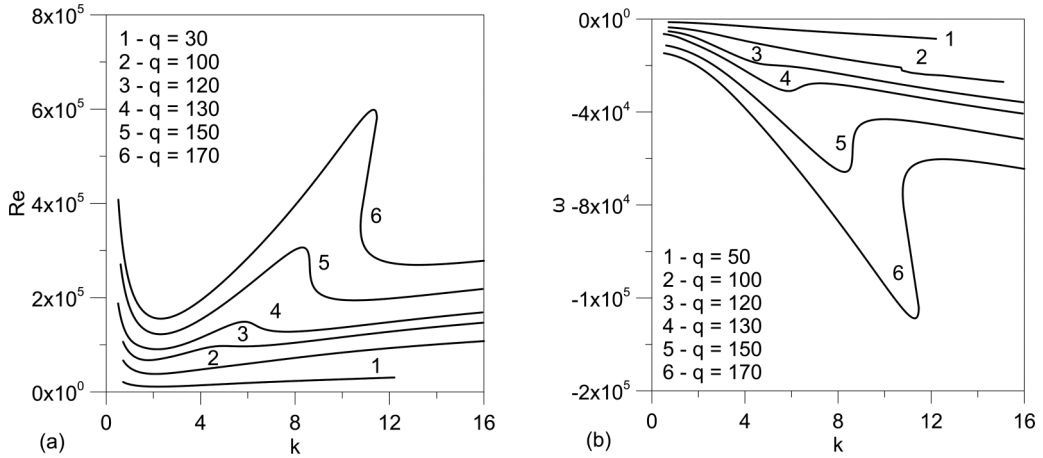

FIG. 3. Neutral stability (a) and dispersion (b) curves in the Brinkman model with the tangential stress jump at the interface for $d = 0.35$ and different values of the parameter q.

occur for the short-wave perturbations which are sharply destabilized when β_{OTW} grows.

B. Darcy-Forchheimer model

Now we turn to the linear stability of the stationary flow in the Darcy-Forchheimer model with tangential velocity jump at the interface. In this case linearized equations for small perturbations are as follows:

$$\frac{\partial \vec{v}}{\partial t} + \mathrm{Re}[(\vec{U}\cdot\vec{\nabla})\vec{v} + (\vec{v}\cdot\vec{\nabla})\vec{U}] = -\vec{\nabla}p + \nabla^2\vec{v}, \tag{44}$$

$$\vec{\nabla}\cdot\vec{v} = 0, \tag{45}$$

$$\frac{\partial \vec{v}}{\partial t} + \mathrm{Re}[(\vec{U}\cdot\vec{\nabla})\vec{v}_p + (\vec{v}_p\cdot\vec{\nabla})\vec{U}] = -\vec{\nabla}p_p - q^2\varphi\vec{v}_p - q\varphi^2 c_F \mathrm{Re}(U_p\vec{v}_p + U_p u_p \vec{e}_x), \tag{46}$$

$$\vec{\nabla}\cdot\vec{v}_p = 0. \tag{47}$$

The equations for the z component of the velocity in pure fluid and in a saturated porous medium are

$$(\lambda + ik\mathrm{Re}U)(w'' - k^2 w) = w^{\mathrm{IV}} - 2k^2 w'' + k^4 w + ik\mathrm{Re}U'' w, \tag{48}$$

$$(\lambda + ik\mathrm{Re}U_p + q^2\varphi + q\varphi^2 c_F \mathrm{Re}U_p)(w_p'' - k^2 w_p) + q\varphi^2 c_F \mathrm{Re}U_p w_p'' = 0. \tag{49}$$

We can introduce the vorticity as in the Brinkman model and reduce the order of (48), but the fourth-order equation for an overlying fluid layer is the well-known Orr-Sommerfeld equation, and it is necessary to compare our problem with classical stability problems.

If we assume the Forchheimer force vanishes, the coefficient at the Laplace operator in (49) equals zero only if the real part of the increment λ is negative, while its imaginary part determined by Re and stationary filtration velocity U_p do not equal zero. This means that there are only damped oscillatory perturbations and the system remains stable. In any other case, this coefficient does not equal zero and we may rewrite Eq. (49) as follows:

$$w_p'' - k^2 w_p = 0. \tag{50}$$

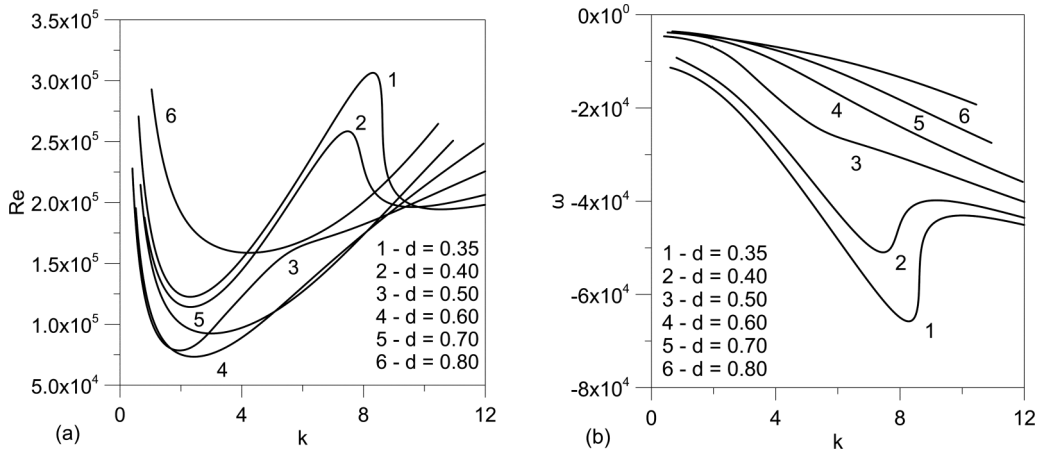

FIG. 4. Neutral stability (a) and dispersion (b) curves in the Brinkman model with the tangential stress jump at the interface for $q = 150(\mathrm{Da} = 4 \times 10^{-5})$ and different values of relative thickness of porous layer d.

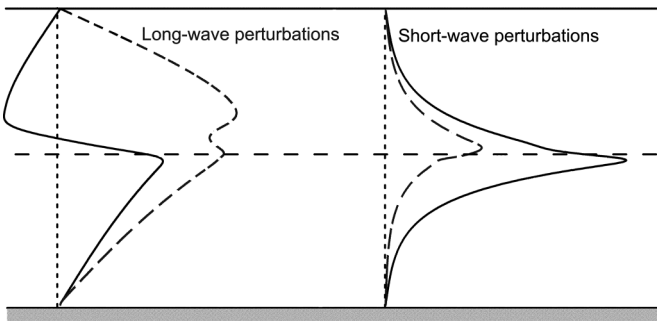

FIG. 5. The profiles of the real (solid) and imaginary (dashed) parts of velocity critical perturbations for long-wave and short-wave modes for the parameter values near to the long-wave and short-wave minima of neutral curve at $d = 0.50, q = 170$.

Moreover, this means that the inertial terms in the porous medium equation do not have an influence on the stability of the system in the Darcy-Forchheimer model. Otherwise, it requires the most accurate analysis when we take into account the nonlinear drag. Eqs. (48) and (50) are completed by the following boundary conditions:

$$z = 1 : w = 0, \quad w'' = 0,$$
$$z = 0 : w_p = 0, \tag{51}$$
$$z = d : w = \varphi w_p, \quad p = p_p, \quad w'' = \alpha_{BJ} q (w' - \varphi w'_p).$$

The pressure continuity condition is rewritten into the relation in terms of velocities from Eqs. (44) and (46) directly.

There exists an exact solution for the velocity perturbations in a porous medium:

$$w_p = \frac{1}{k}(\sinh kz \cos k\varepsilon z + i \cosh kz \sin k\varepsilon z), \tag{52}$$

where

$$\varepsilon = \frac{c_F \varphi \mathrm{Re}^2 k^2}{8q^7(\lambda + q^2\varphi)},$$

and the normalization factor $1/k$ is determined in such a way as to simplify further calculations. Generally, it is arbitrary due to the equation's linearity. The parameter ε is an imaginary part of the eigenvalue of (49) simplified at large λ, Re, and q. Its typical value is less than 10^{-9}, because λq^7 is in the denominator. Therefore, the Forchheimer force's influence on flow stability is negligible.

Taking into account the solution (52) we transform the linear stability problem for the two-layer system to the standard Orr-Sommerfeld equation [34,35] for the flow in a layer with a free undeformable upper boundary and unusual conditions at the lower boundary:

$$z = d : w = \frac{\varphi}{k} \sinh kd + i\varphi\varepsilon d \cosh kd, \quad p = p_p,$$
$$w'' = \alpha_{BJ} q (w' - \varphi \cosh kd)$$
$$- i\alpha_{BJ} q \varepsilon \varphi (\cosh kd + kd \sinh kd). \tag{53}$$

Here is the full form of these conditions. Actually, one can exclude the terms with ε because its value is vanishingly small, and the calculated changes of critical Reynolds numbers and eigenfrequencies are within the accuracy of the algorithm. The Forchheimer force effect is determined only by stationary velocity change. The stability problem was solved numerically by the shooting method based on calculation of the fundamental system solution with step-by-step orthogonalization of the solution vectors [32,33].

The neutral and dispersion curves for the Darcy and Darcy-Forchheimer models at $d = 0.35$ and different values of the porous matrix permeability are presented in Fig. 7. The results for fixed permeability ($q = 700, \mathrm{Da} = 2 \times 10^{-6}$) and different thicknesses of the porous layer d are shown in Fig. 8. It is seen that the permeability decrease stabilizes the system as in the previous model. However, the short-wave minimum corresponds here to the most dangerous perturbations in the whole parameter range. The qualitative dependence of the stability properties on d is the same as in the Brinkman model. The minima of the neutral curve merge with d growth.

The nonlinear Forchheimer drag force does not change the neutral stability curves in the plot scale [see Fig. 7(a)]. The critical frequency difference is less than 2% and perceptible only for the large wave number [Fig. 7(b)]. The detailed analysis of Forchheimer drag force influence on the flow stability in the Brinkman model is presented in Sec. III C.

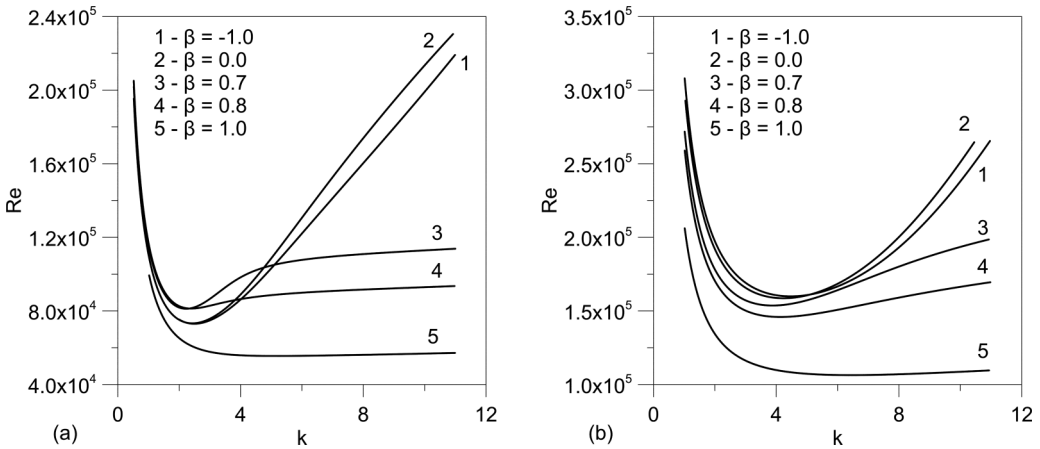

FIG. 6. Neutral stability curves for the Brinkman model with the tangential stress jump at the interface at $q = 150(\mathrm{Da} = 4 \times 10^{-5})$ and different values of the parameter β_{OTW} in the boundary conditions (a) $d = 0.6$, (b) $d = 0.8$; the β_{OTW} is written as β at the figures.

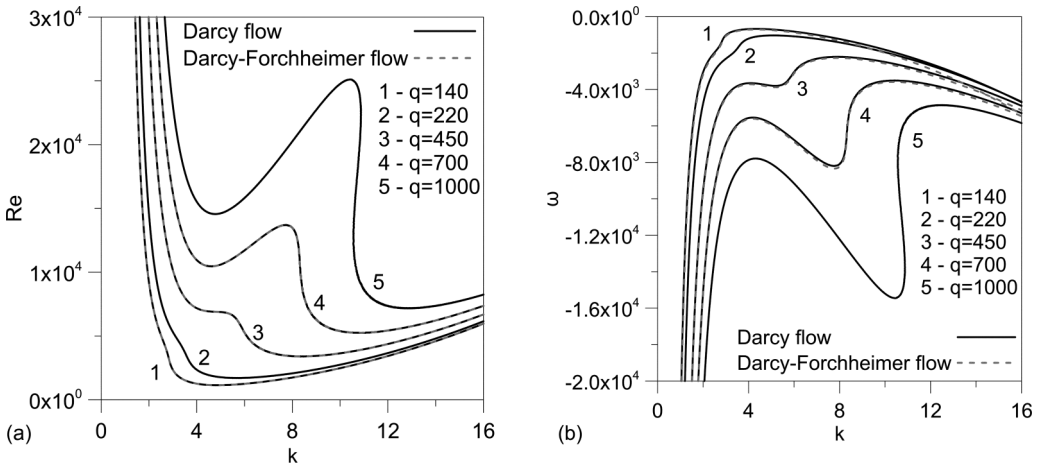

FIG. 7. Neutral stability (a) and dispersion (b) curves in the Darcy and Darcy-Forchheimer models for $d = 0.35$, $\alpha_{\mathrm{BJ}} = 1$ and different values of the parameter q.

Figure 9 shows the structure of the velocity critical perturbations for long-wave and short-wave modes of the Darcy model. The profiles obtained for the parameter values close to the long-wave and short-wave minima of the neutral curve at $d = 0.50, q = 700$ are plotted.

The parameter α_{BJ} in the Beavers and Joseph boundary condition has a very strong influence on the system stability (Fig. 10). The increase of α_{BJ} reduces the tangential stationary velocity jump at the interface [see Fig. 2(b)] and the main destabilizing factor is weakened. The neutral stability curves prove it. The increase of α_{BJ} leads the long-wave minimum appearance but this minimum is not dominating in the parameter range under consideration.

Critical Reynolds numbers in the Darcy model are 100 times lower than in the Brinkman model (Fig. 11) due to the velocity jump at the interface.

C. Influence of Forchheimer force on flow stability

Introducing the nonlinear drag force in the Darcy equations does not change the instability threshold, while the critical frequency increases by less than 2% (see Fig. 7). Thus, the Darcy and Darcy-Forchheimer models are equivalent in the considered problem.

In the case of the Brinkman model, we have shown that accounting for the quadratic drag force can be reduced to the rescaling of Re and q with keeping the same form of the neutral stability curves as in Sec. III A.

The extension of Eq. (9) by introducing the Forchheimer force is [1]

$$\frac{\partial \vec{v}_p}{\partial t} + \mathrm{Re}(\vec{v}_p \cdot \vec{\nabla})\vec{v}_p = -\vec{\nabla} p_p - q^2 \varphi \vec{v}_p - \varphi^2 c_F q \mathrm{Re}|\vec{v}_p|\vec{v}_p + \nabla^2 \vec{v}_p - \frac{1}{\sin\alpha}\vec{\gamma}. \tag{54}$$

An additional nonlinear term appears also in the boundary condition for the tangential stresses at the interface (12):

$$z = d : \frac{\partial v_x}{\partial z} - \varphi \frac{\partial v_{px}}{\partial z} = -\beta_{\mathrm{OTW}} q \varphi v_{px} + \beta_F \varphi^2 \mathrm{Re}|v_{px}|v_{px}, \tag{55}$$

where $\beta_F = c_F \delta K^{-1/2}$ is the additional dimensionless parameter determined by the porous medium properties and the viscous boundary layer thickness δ near the interface.

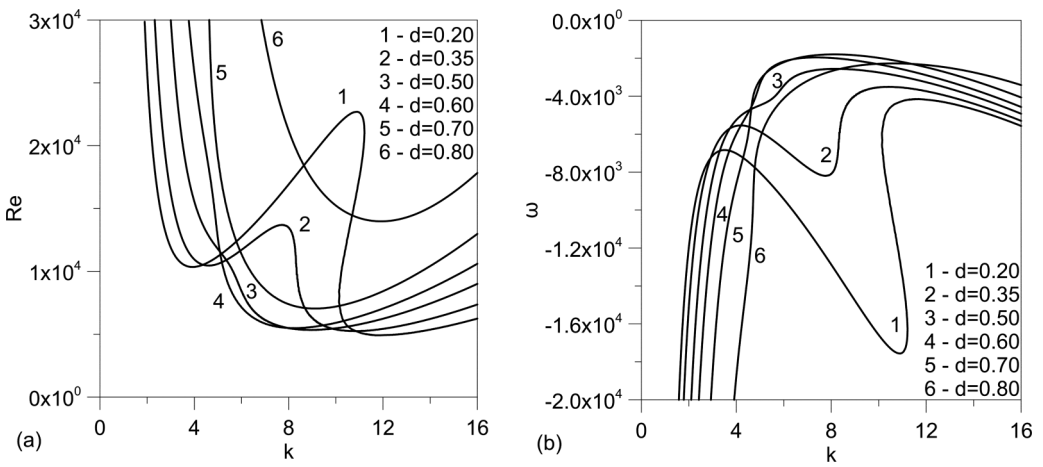

FIG. 8. Neutral stability (a) and dispersion (b) curves in the Darcy and Darcy-Forchheimer models for $q = 700(\mathrm{Da} = 2 \times 10^{-6})$ and different values of relative thickness of porous layer d.

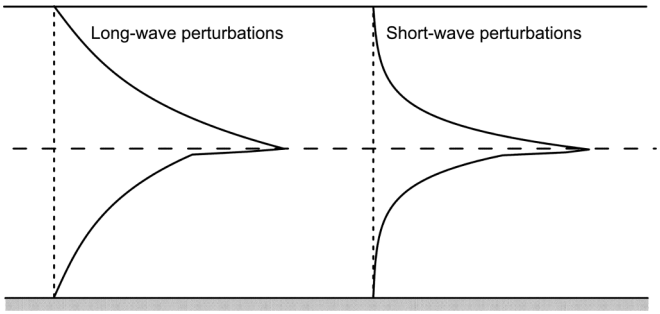

FIG. 9. The profiles of the real parts of velocity critical perturbations for long-wave and short-wave modes for the parameter values near to the long-wave and short-wave minima of the neutral curve at $d = 0.50, q = 700$.

First, we consider the stationary solution of the transformed Brinkman-Forchheimer system (7), (8), (10), and (54). It cannot be obtained analytically. Therefore, we analyze it assuming that the quadratic drag force is small relative to the other equation terms. Introducing the corrections u and u_p to the stationary flow, one can rewrite the stationary equations in the form

$$U'' + u'' + 1 = 0, \tag{56}$$

$$U_p'' + u_p'' - q^2(U_p + u_p) + 1 = q\varphi^2 c_F \mathrm{Re}(U_p + u_p)^2. \tag{57}$$

With (24) and (26) the linearized equations and boundary conditions for the corrections are as follows:

$$u'' = 0, \tag{58}$$

$$u_p'' - q^2\varphi(1 + 2c_F q^{-1}\varphi \mathrm{Re} U_p)u_p = c_F q^{-1} r \mathrm{Re} U_p^2, \tag{59}$$

$$\begin{aligned} &z = 1 : u' = 0, \\ &z = 0 : u_p = 0, \\ &z = d : u = \varphi u_p,\ \ u' - u'_p = -\beta q \varphi u + \varphi^2 \beta_F \mathrm{Re} U_p u_p, \end{aligned} \tag{60}$$

where $r = q\varphi^{1/2}$.

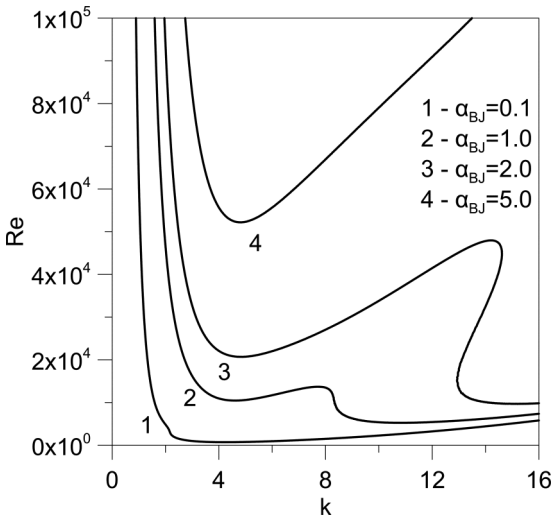

FIG. 10. Neutral stability curves in the Darcy model for $q = 700(\mathrm{Da} = 2 \times 10^{-6}), d = 0.35$, and different values of α_{BJ}.

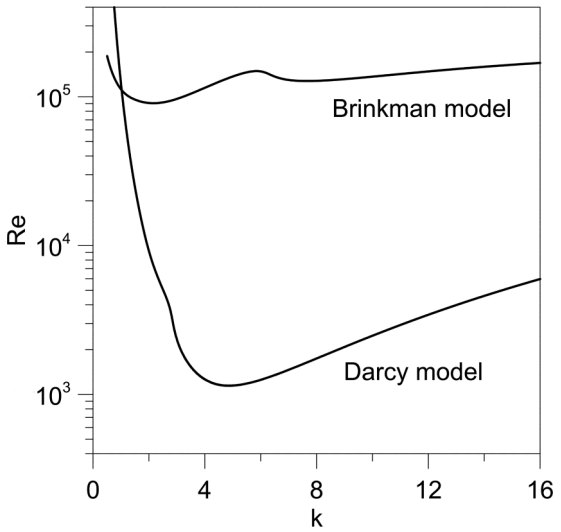

FIG. 11. Comparison of the neutral curves in the Brinkman and Darcy models for $q = 140(\mathrm{Da} = 5 \times 10^{-5}), d = 0.35, \alpha_{\mathrm{BJ}} = 1$, and $\beta_{\mathrm{OTW}} = 0$.

For estimates of the velocity change we can apply the average value of U_p:

$$\langle U_p \rangle \sim \frac{2}{r^2}. \tag{61}$$

Besides, there is another characteristic velocity is the average filtration velocity in the boundary layer δ:

$$\langle U_p \rangle \sim \frac{1}{2r}. \tag{62}$$

These values bound the true value of average velocity from below and above. They also give the limiting estimates for the stationary velocity correction. The lower bound gives

$$u_p > -\frac{4c_F \mathrm{Re}}{q^5\varphi}(1 - \mathrm{e}^{-rz}), \quad u > -4\frac{c_F \mathrm{Re}}{q^5\varphi}, \tag{63}$$

while the corrections at the upper bound are as follows:

$$u_p < -\frac{c_F \mathrm{Re}}{4q^3}(1 - \mathrm{e}^{-rz}), \quad u < -\varphi\frac{c_F \mathrm{Re}}{4q^3}. \tag{64}$$

The corrections are negative because the nonlinear drag force decelerates the main flow. Taking into account the typical critical values of Re and q, one can see that the corrections are negligible for $q \sim 10^2$.

The additional terms in the governing equation also change the stability problem formulation. It needs a particular analysis. It is possible to show that the problem can be reduced to the previous system (39)–(42) by rescaling the parameter q. The equation (41) for the flow vorticity in the porous layer transforms into the following equation:

$$\begin{aligned} &\lambda\Omega_p + \mathrm{Re}(ikU_p\Omega_p + w_p U''_p) \\ &\quad = -q^2\varphi\Omega_p + \Omega''_p - k^2\Omega_p \\ &\qquad - \varphi c_F q \mathrm{Re}(\varphi U_p\Omega_p - U'_p w'_p), \end{aligned} \tag{65}$$

and the boundary conditions at the interface may be rewritten as

$$(\lambda + 2k^2)(w' - w'_p) + ik\mathrm{Re}[(Uw' - U_p w'_p) - (U'w - U'_p w_p)] + ik(\Omega' - \Omega'_p) = (q^2\varphi + \varphi^2 c_F q \mathrm{Re} U_p) w'_p, \quad (66)$$

$$ik(\Omega - \Omega_p) - k^2(w - w_p) = \beta_{\mathrm{OTW}} q\varphi w'_p - \varphi^2 \beta_F \mathrm{Re} U_p w'_p. \quad (67)$$

It is possible to estimate the magnitude of terms in (65)–(67) for large q. Taking typical values $\varphi \sim 0.5$,q $\sim 10^2$, and $d \sim 0.5$, we obtain

$$U''_p \mathrm{Re} \sim q\mathrm{Re}, \quad |ik\mathrm{Re}U_p| \sim kq^{-1}\mathrm{Re}, \quad |c_F\varphi^2 q\mathrm{Re}U'_p| \sim 10^{-1} q\mathrm{Re}. \quad (68)$$

The Forchheimer drag force is smaller than the other terms. Neglecting $c_F\varphi^2 q\mathrm{Re}U'_p w'_p$ in Eq. (65) and rescaling q, we transform (65) to (41) again. Using the estimate (61) for average filtration velocity, we get the lower bound for this value of q:

$$\tilde{q}^2 \approx q^2\left(1 + \frac{2c_F\mathrm{Re}}{q^3}\right) \sim q^2(1 + q^{-3}\mathrm{Re}), \quad (69)$$

and average velocity limit (62) provides its upper bound:

$$\tilde{q}^2 \approx q^2\left(1 + \frac{c_F\mathrm{Re}}{4q^2}\right) \sim q^2(1 + 10^{-1}q^{-2}\mathrm{Re}). \quad (70)$$

The boundary conditions (66) and (67) permit a similar q scaling. In this case the condition (66) is not changed while the small corrections of the order of $O(q^{-3}\mathrm{Re})$ or $O(10^{-1}q^{-2}\mathrm{Re})$ arise in the condition (67) in the first and second cases, respectively. Such corrections arise in all the terms including the stationary filtration flow velocity. The estimates (69) and (70) bound the true value of $\tilde{q}$.

Thus, the equations and boundary conditions are not changed in the leading order, while the q slightly increases. This means that all the stability properties and previous results (Sec. III A) are also not changed. Nonlinear drag force produces the effective increase of q (or permeability decrease) and the corresponding change of the critical Re. The limiting estimates of corrected value of Re are obtained from the interpolation and extrapolation of the neutral curves for the Brinkman model (see Fig. 5) by q, and are listed in Table I for some values of the system parameters. One sees that the nonlinear Forchheimer force stabilizes the flow due to additional perturbation damping at the interface.

TABLE I. Critical Reynolds number in the Brinkman model without (B) and with (F) Forchheimer force for the long-wave (lw) and short-wave (sw) instability modes.

q			$10^{-4}\mathrm{Re}_{\mathrm{lw}}$			$10^{-4}\mathrm{Re}_{\mathrm{sw}}$		
B	min, F	max, F	B	min, F	max, F	B	min, F	max, F
100	102	119	3.82	4.07	6.87			
120	122	147	6.74	7.53	11.7	9.66	10.3	18.7
130	133	163	9.06	9.30	14.4	12.8	13.9	24.3
150	153	188	12.2	12.7	18.7	19.4	20.8	33.1
170	173	213	15.5	16.1	22.9	27.0	27.7	41.6

IV. DISCUSSION: PHYSICAL MECHANISMS OF INSTABILITY

Let us discuss the results of the linear stability study obtained within the different filtration models.

The common feature of the results is the bimodality of neutral stability curves. There exist long-wave and short-wave minima. The dimensionless wave number of long-wave perturbations in both models varies weakly with the parameter change (see Figs. 3 and 4). In the Brinkman model this mode corresponds to the large-scale vortices occupying the whole system (see Fig. 5, left). It means that these perturbations are "inviscid" and satisfy the Rayleigh inflection point theorem, despite the whole velocity profile not being smooth. One can see the inflection point lies in the porous layer. Therefore, these "inviscid" critical motions occupy both fluid and porous layers.

The short-wave critical motions in the Brinkman model are localized near the layer interface (see Fig. 5, right). Their critical Re has a strong dependence on wave number that means high influence of the fluid viscosity on perturbations development. It can be a result of the drag force gradient changes in the fluid layer. It is proportional to (dU/dz) and increases from the top surface to the bottom, and has a maximum value near the interface [see stationary velocity profile, Fig. 2(a)].

The main physical mechanism of the instability in the Darcy-Forchheimer model is the same as for Kelvin-Helmholtz instability. The tangential velocity jump at the interface [see Fig. 2(b)] is the leading reason for the instability. Long-wave perturbations are damped by the gravity force, while the drag force in the porous layer exerts the short-wave perturbation damping for $k > 10$. In classical Kelvin-Helmholtz instability, the short-wave perturbations are damped by surface tension [36]. The critical wave number of small-scale vortices is highly sensitive to the parameter change. It grows when the permeability decreases due to the drag force increase (see Fig. 7). As in the case of the Brinkman model, in the system with the Darcy-Forchheimer porous medium the long-wave critical motions occupy both the fluid layer and porous layer, and short-wave critical motions are localized near the layer interface (see Fig. 9).

For the Brinkman model the long-wave instability is dominating at $q < 200$ while the short-wave instability related to the small-scales vortices localized near the interface may develop in a low-permeability porous medium. Contrary to that, for the Darcy-Forchheimer model the short-wave perturbations are critical over the entire parameter range under consideration. This corresponds to the results from [2].

The increase of porous layer thickness destabilizes the system at $d < 0.6$ and stabilizes it when $d > 0.6$ in both Brinkman and Darcy models. The short-wave minimum is the most sensitive to d variations. To explain this one should analyze the perturbations damping in the porous layer. The structure of the eigenfunctions (see Fig. 5) shows that the perturbations are localized in the pure fluid layer for small

d and in the porous layer for large d. In the first case, a thin boundary layer is formed in the porous medium and the velocity in the wider, pure fluid layer increases. This leads to a rapid change of the velocity and a strong effect of the viscosity in the transition layer near the interface. As the result, the perturbations damping is significant and the flow is more stable than in the case of larger d. On the other hand, the growth of d decreases the absolute value of the velocity in the overlying fluid, and this stabilizes the system. Thus, the balance of two stabilization mechanisms may provide the minimum of critical Reynolds number at some intermediate value of d.

There exists only oscillatory instability. This leads to the formation of traveling waves. The results of the direct numerical simulation of the waves at the interface of layers are presented in [23]. The simulation is performed for full nonlinear equations. The two-layer system is described by a one-equation model with nonuniform permeability and porosity.

The two filtration models which we implemented give different results. The stationary flow in the Brinkman model with the boundary conditions by Ochoa-Tapia and Whitaker at the interface is more stable than that in the Darcy model. The critical Reynolds number that we obtained using the Brinkman model is in good agreement with the results obtained in [4] for the three-layer system of fluid between two porous layers with the collocation method based on Chebyshev polynomials. A tangential stress jump leads to the break of the stationary velocity profile; the transition boundary layer between the pure fluid and saturated porous medium is thin and poorly determined [see Fig. 2(a)]. The velocity profile becomes smoother with q increase; this stabilizes the stationary plane-parallel flow.

In the Darcy and Darcy-Forchheimer models with the boundary conditions by Beavers and Joseph the stationary flow is less stable because of the tangential velocity jump near the interface [see Fig. 2(b)]. The jump magnitude is determined by the parameter α_{BJ}. Its growth stabilizes the flow and produces a strong increase of the short-wave minimum. The critical Reynolds numbers in the Darcy model are 100 times smaller than in the Brinkman model.

Finally, the estimation of the nonlinear drag force (Forchheimer term) effect on the stationary flow stability shows that it is insignificant in both Darcy and Brinkman filtration models. The corrections to the neutral curves in the Brinkman model permit estimating the interval bounding the critical Reynolds number. The Forchheimer force stabilizes the flow.

V. CONCLUSIONS

A numerical study of linear stability of plane-parallel flow of an incompressible viscous fluid flowing down the porous layer saturated by the same fluid is studied in the framework of different filtration models. The neutral stability curves, the values of critical Reynolds numbers, and frequencies of critical perturbations are calculated. The eigenfunctions of the problem are obtained.

The common features of the stationary flow instability are investigated. The possible physical reasons for the dependence of critical conditions on the parameters and for the qualitative difference in the results obtained within the Brinkman and Darcy-Forchheimer models are discussed. Parameters of the two-layer system are chosen in such a way that the system can be described equally by both of these models: the porous medium has high porosity and the pore-scale Reynolds number is small enough to provide sufficient accuracy for the Darcy and Darcy-Forchheimer laws.

The influence of the boundary conditions at the interface and of the stationary flow structure on the perturbations localization within the layer is discussed. The long-wave instability minimum is found to be dominating in the Brinkman model and the short-wave instability minimum in the Darcy model. The latter is related to the tangential velocity jump as in the classical Kelvin-Helmholtz instability. The critical Reynolds numbers in the Darcy model are sufficiently lower than those in the Brinkman model, which is also related to the tangential velocity jump for the Darcy model.

Experimental study of the stability of stationary flow is recommended as an efficient method for the verification of different theoretical models.

ACKNOWLEDGMENT

The work was financially supported by the Russian Foundation for Basic Research (Grant No. 12-01-00795).

[1] D. A. Nield and A. Bejan, *Convection in Porous Media*, 4th ed. (Springer, New York, 2013), p. 778.

[2] A. A. Hill and B. Straughan, Poiseuille flow in a fluid overlying a highly porous material, Adv. Water Resour. **32**, 1609 (2009).

[3] A. S. Berman, Laminar flow in channels with porous walls, J. Appl. Phys. **24**, 1232 (1953).

[4] N. Tilton and L. Cortelezzi, Linear stability analysis of pressure-driven flows in channels with porous walls, J. Fluid Mech. **604**, 411 (2008).

[5] K. Gavrilov, G. Accary, D. Morvan, D. Lyubimov, S. Méradji, and S. Bessonov, Numerical simulation of coherent structures over plant canopy, Flow, Turbul. Combust. **86**, 89 (2011).

[6] M. Ghisalberti and H. Nepf, The structure of the shear layer in flows over rigid and flexible canopies, Environ. Fluid Mech. **6**, 277 (2006).

[7] M. le Bars and M. G. Worster, Interfacial conditions between a pure fluid and a porous medium: Implications for binary alloy solidification, J Fluid Mech. **550**, 149 (2006).

[8] E. A. Kolchanova, D. V. Lyubimov, and T. P. Lyubimova, The onset and nonlinear regimes of convection in a two-layer system of fluid and porous medium saturated by the fluid, Transp. Porous Media **97**, 25 (2013).

[9] C. Yin, C. Fu, and W. Tan, Stability of thermal convection in a fluid-porous system saturated with an Oldroyd-B fluid heated from below, Transp. Porous Media **99**, 327 (2013).

[10] M. S. Muddamallappa, D. Bhatta, and D. N. Riahi, Numerical investigation on marginal stability and convection with and without magnetic field in a mushy layer, Transp. Porous Media **79**, 301 (2009).

[11] D. Bhatta, M. S. Muddamallappa, and D. N. Riahi, On perturbation and marginal stability analysis of magneto-convection in active mushy layer, Transp. Porous Media **82**, 385 (2010).
[12] S. Govender, Stability of solutal convection in a rotating mushy layer solidifying from a vertical surface, Transp. Porous Media **90**, 393 (2011).
[13] S. P. Suma, Y. H. Gangadharaiah, R. Indira, and I. S. Shivakumara, Throughflow effects on penetrative convection in superposed fluid and porous layers, Transp. Porous Media **95**, 91 (2012).
[14] B. Alazmi and K. Vafai, Analysis of fluid flow and heat transfer interfacial conditions between a porous medium and a fluid layer, Int J. Heat Mass Transfer **44**, 1735 (2001).
[15] D. V. Lyubimov and I. D. Muratov, On convective instability of fluid in layered system, in *Hydrodynamics* (Perm State Pedagogic Institute, Perm, Russia, 1977), Vol. 10, pp. 38 (in Russian).
[16] F. Chen and C. F. Chen, Onset of finger convection in a horizontal porous layer underlying a fluid layer, J. Heat Transfer **110**, 403 (1988).
[17] J. A. Ochoa-Tapia and S. Whitaker, Momentum transfer at the boundary between a porous medium and a homogeneous fluid-I. Theoretical development, Int. J. Heat Mass Transfer **38**, 2635 (1995).
[18] J. A. Ochoa-Tapia and S. Whitaker, Momentum transfer at the boundary between a porous medium and a homogeneous fluid—II. Comparison with experiment, Int. J. Heat Mass Transfer **38**, 2647 (1995).
[19] G. S. Beavers and D. D. Joseph, Boundary conditions at a naturally permeable wall, J. Fluid Mech. **30**, 197 (1967).
[20] M Minale, Momentum transfer within a porous medium. I. Theoretical derivation of the momentum balance on the solid skeleton, Phys. Fluids **26**, 123101 (2014).
[21] M. Minale, Momentum transfer within a porous medium. II. Stress boundary condition, Phys. Fluids **26**, 123102 (2014).
[22] B Berkowitz, Boundary conditions along permeable fracture walls: Influence on flow and conductivity, Water Resour. Res. **25**, 1919 (1989).
[23] M. A. M. van Lankveld, Validation of boundary conditions between a porous medium and a viscous fluid, Ph.D. thesis, Eindhoven University of Technology, 1991.
[24] A. A. Hill and B Straughan, Poiseuille flow in a fluid overlying a porous medium, J. Fluid Mech. **603**, 137 (2008).
[25] T. P. Lyubimova, D. T. Baydina, and D. V. Lyubimov, Stability and nonlinear regimes of flow over a saturated porous medium, Nonlinear Processes Geophys. **20**, 543 (2013).
[26] P. D. Antonladis and M. V. Papalexandris, Dynamics of shear layers at the interface of a highly porous medium and a pure fluid, Phys. Fluids **27**, 014104 (2015).
[27] A. Hong, M. Tao, and A Kudrolli, Onset of erosion of a granular bed in a channel driven by fluid flow, Phys. Fluids **27**, 013301 (2015).
[28] C. Varsakelis and M. V. Papalexandris, Numerical simulation of subaqueous chute flows of granular materials, Eur. Phys. J. E **38**, 40 (2015).
[29] N. Martys, D. P. Bentz, and E. J. Garboczi, Computer simulation study of the effective viscosity in Brinkman equation, Phys. Fluids **6**, 1434 (1994).
[30] H. C. A. Brinkman, Calculation of the viscous force exerted by a flowing fluid on a dense swarm of particles, Appl. Sci. Res. A **1**, 27 (1947).
[31] A. Mikelić and W. Jäger, On the interface boundary condition of Beavers, Joseph, and Saffman, SIAM J. Appl. Math. **60**, 1111 (2000).
[32] S. D. Conte, The numerical solution of linear boundary value problems, SIAM Rev. **8**, 309 (1966).
[33] S. K. Godunov, Numerical solution of boundary-value problems for systems of linear ordinary differential equations, Usp. Mat. Nauk **16**, 171 (1966) (in Russian).
[34] W. M. F. Orr, The stability or instability of the steady motions of a perfect liquid and of a viscous liquid. Part II: A viscous liquid, Proc. R. Ir. Acad., Sect. A **27**, 69 (1907).
[35] C. C. Lin, *The Theory of Hydrodynamic Stability* (Cambridge University Press, Cambridge, 1966), p. 155.
[36] W. Thomson (Lord Kelvin), *Mathematical and Physical Papers.* Vol. 4. Hydrodynamics and General Dynamics (Cambridge University Press, Cambridge, 1910), p. 563.